IN-SITU DETERMINATION OF DYNAMIC STIFFNESS FOR RESILIENT ELEMENTS

Authors: J.W.R. Meggitt[1*] , A. S. Elliott[1], A. T. Moorhouse[1] and Kevin H. Lai[2]

1) Acoustics Research Centre, University of Salford, Greater Manchester, United Kingdom

2) The Boeing Company, Seattle, Washington, United States

Contact: j.w.r.meggitt@edu.salford.ac.uk

Abstract An in-situ method for the measurement of a resilient elements dynamic transfer stiffness is outlined and validated. Unlike current methods, the proposed in-situ approach allows for the characterisation of a resilient element whilst incorporated into an assembly, and therefore under representative mounting conditions. Potential advantages of the proposed method include the simultaneous attainment of both translational and rotational transfer stiffness components over a broad frequency range without the need for any cumbersome test rigs. These rotational components are obtained via the application of a finite difference approximation. A further advantage is provided via an extension to the method allowing for the use of remote measurement positions. Such an extension allows for the possible characterisation of hard-to-reach elements, as well as the over-determination of the problem. The proposed method can thus be broken into two sub-methods; direct and remote. Preliminary results are shown for the direct method on a simple mass-isolator-mass laboratory test rig along with a more realistic beam-isolator-plate system. Validation of this method is provided for by a transmissibility prediction, in which an obtained dynamic stiffness value is used to predict the transmissibility of a separate system. Further results are presented for the remote case using a beam-isolator-plate system. In all cases the results are obtained over a substantial frequency range and are of a sufficient quality to be used as part of structure borne sound and vibration predictions.

1 Introduction

The work presented in this paper concerns the development of an in-situ measurement method for the attainment of the dynamic transfer stiffness for resilient elements/isolators [1]. The need for such a method has been driven by its potential use in the field of substructure synthesis and the prediction of structure-borne sound and vibration.

Often when predicting structure-borne sound and vibration it is convenient to model an assembly in such a way that the frequency response functions (FRFs) of the individual subsystems are obtained independently, then coupled together mathematically. This method is referred to as 'substructure synthesis'. Whilst the concept itself dates back as far as the 1960s [2, 3], only in more recent years, with advancements in data acquisition has this technique become a useful tool in experimental vibroacoustics [4–6]. An important requirement for this substructuring methodology is that the FRF's of the individual subsystems are obtained in a transferable manner, i.e. they are solely properties of the subsystem. For source and receiver subsystems this is not such a problem as their FRFs may be obtained experimentally through an approximated 'free' suspension or generated numerically using modelling techniques such as FEA. Unfortunately the independent property required for the characterisation of a resilient element, the dynamic transfer stiffness [7], is not so easily attained. Current methods [8–11] including international standards [12–15] not only require cumbersome test rigs which necessitate that the resilient elements be removed from its assembly, but their applications are generally limited to low frequencies. It is therefore the aim of this paper to provide a convenient and flexible method that allows for the dynamic transfer stiffness to be obtained in-situ and over a considerable frequency range.

2 Dynamic Stiffness

Consider the SIR (source-isolator-receiver) system shown in figure 1, where by the subsystem I may be made up of multiple isolators. If we consider the source inactive, the transfer impedance across I is defined as,

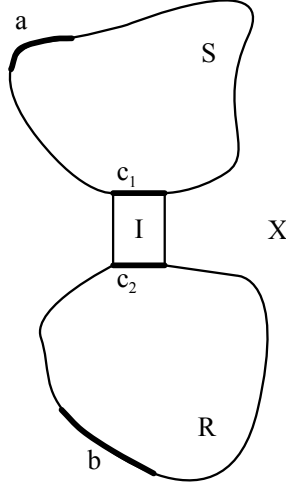$$\bar{f}_{c_2} = \mathbf{Z}_{c_2 c_1} v_{c_1} \tag{1}$$

Figure 1: General source isolator receiver system.

where $\bar{\mathrm{f}}_{\mathbf{c_2}}$ is the blocked force vector (with $\bar{\ }$ denoting the blocked condition) at interface c_2, $\mathrm{v}_{\mathbf{c_1}}$ is an applied velocity vector at interface c_1 and $\mathbf{Z}_{\mathbf{c_2c_1}}$ is the transfer impedance matrix relating these two quantities [16]. The blocked condition at c_2 removes the effect of the receiver structure on the transfer impedance, similarly, an applied velocity at c_1 is applied irrespective of the source structures passive response. We can therefore assume that the transfer impedance is independent of both the source and receiver and is solely a property of the isolator. The transfer impedance $\mathbf{Z}_{\mathbf{c_2c_1}}$ may be obtained through the inversion of a measured contact interface mobility matrix

$$\left[\begin{array}{cc} \mathbf{Z}_{\mathbf{c_1c_1}} & \mathbf{Z}_{\mathbf{c_1c_2}} \\ \mathbf{Z}_{\mathbf{c_2c_1}} & \mathbf{Z}_{\mathbf{c_2c_2}} \end{array} \right] = \left[\begin{array}{cc} \mathbf{Y}_{\mathbf{c_1c_1}} & \mathbf{Y}_{\mathbf{c_1c_2}} \\ \mathbf{Y}_{\mathbf{c_2c_1}} & \mathbf{Y}_{\mathbf{c_2c_2}} \end{array} \right]^{-1}. \tag{2}$$

The dynamic transfer stiffness, relating force to displacement rather than velocity, may be obtained by multiplying $\mathbf{Z}_{\mathbf{c_2c_1}}$ through by $i\omega$

$$i\omega \mathbf{Z}_{\mathbf{c_2c_1}} = \mathbf{K}_{\mathbf{c_2c_1}}. \tag{3}$$

The above method harbours no limitations with regards to the impedance of the coupling element, providing that it is linear and time invariant. That is to say that the same method can, and has in the past, been used to obtain the transfer stiffness/impedance of a portion of a rigid assembly with good results. Moreover, the method is not restricted to use on resilient elements under linear compression and may be applied to elements under

any level of pre-load providing that the applied forces during operation remain locally linear. An alternative derivation of the method outlined above may be formulated from a more theoretical standpoint, although with the aim of keeping this paper focused on the methods application this has not been included. However for those interested it will likely form the basis of a future paper.

In order to demonstrate the independent nature of the dynamic transfer stiffness, the contact interface mobility matrices of two mass-isolator-mass (M-I-M) assemblies have been measured. A spaced pair configuration was used, as shown by figure 2. Averaging the mobilities above and below the mount provides an approximate single contact point interface mobility matrix. In general this mobility matrix may or may not be made up of sub-matrices accounting for multiple degrees of freedom. However, the particular measurement configuration used here limits the determinable dynamic transfer stiffness's to the out-of-plane z degree of freedom only. Consequently the sub-matrices are reduced to scalar quantities.

Two different sets of masses were used in the construction of the two test rigs (source masses were chosen such that they were sufficiently different without introducing any preload effects in the isolator). Details of the source and receiver masses are summarised in table 1. The transfer mobility and dynamic stiffness's obtained from these two test rigs are shown in figure 3.
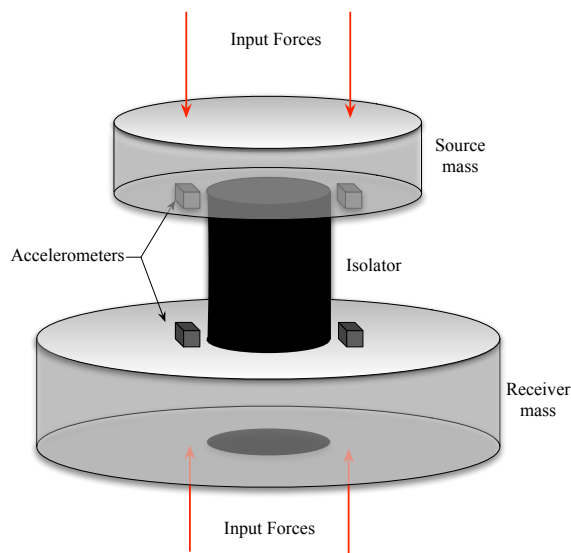

Figure 2: Mass-Isolator-Mass test rig.

4

Comparing the mobility results from figure 3 for the two test rigs it is clear that an increase in the inertia of the source and receiver structures causes a significant decrease in the transfer mobility $Y_{c_2 c_1}$, as expected. However as suspected, the dynamic transfer stiffness, $K_{c_2 c_1}$, remains unchanged by this variation. We can thus confirm that the dynamic transfer stiffness obtained through the inversion of a measured contact interface mobility matrix is in fact an independent isolator quantity. It should be noted that the noise introduced at higher frequencies (above $\approx$ 2kHz) is a result of the isolator attenuated vibration falling below the sensitivity threshold of the measurement equipment. The frequency at which this noise is introduced is dependent on the inertia of the assembly, with a larger mass requiring a larger vibration amplitude in order to exceed the sensitivity threshold.
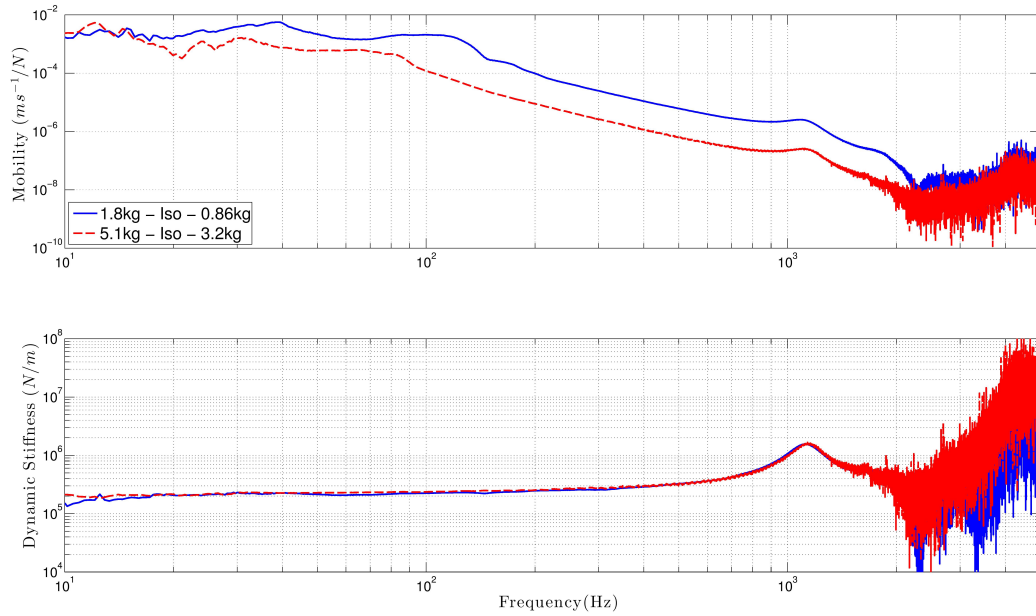

Figure 3: Results obtained from test rigs 1 & 2. Upper - transfer mobilities. Lower - dynamic transfer stiffness's.

	Source	Isolator	Receiver
Test rig 1	0.86kg mass		1.8kg mass
Test rig 2	3.2kg mass		5.1kg mass
Test rig 3	0.86kg mass	Continental	3.2kg mass
Test rig 4	0.86kg mass	CONTITECH	5.1kg mass
Test rig 5	0.86kg mass	27 796 25 - 29	18.3kg mass
Test rig 6	Steel beam(mm) 250L x 50W x 9D		Perspex plate(mm) 340L x 495W x 10D

Table 1: Test rig construction details.

It may be of interest to note that the resilient mount used above, and throughout the rest of this paper is a 'SCHWINGMETALL Compression Mount, C Type, Mould Number 27796/C' and is supplied with a static spring stiffness of 16800N/m. Comparing this to the measured value at 10Hz of ≈ 20000N/m, it is not unreasonable to put the 19% increase in stiffness down to the frequency dependent nature of rubber like materials. Furthermore this increase in stiffness over just 10Hz provides a strong rational behind the use of a dynamic measure of the stiffness of resilient mounts and isolators.

2.1   Transmissibility Validation

It has so far been shown that the dynamic transfer stiffness is an independent quantity and can be obtained through a simple matrix inversion, however the validity of the resulting stiffness has not yet been established. Such confirmation will be achieved in the following section by means of a transmissibility prediction. The transmissibility of a given single degree of freedom system may be obtained either experimentally through the ratio of operational velocities above and below the mount, equation 4, or theoretically using a simplified model, i.e. a mass on a spring, equation 5,

$$T_{\text{meas}} = \frac{v_{\text{in}}}{v_{\text{out}}} = \frac{Y_{c_1 c_1}}{Y_{c_2 c_1}} \tag{4}$$

and

$$T_{\text{pred}} = \frac{Z_s}{Z_m + Z_s} \tag{5}$$

The validation process undertaken may be outlined as follows:

1 A mass-isolator-mass test rig is constructed, with a source mass of M_1.

2 A set of forces are applied above and below the mount, and the resulting interface mobility matrix inverted to yield the dynamic transfer stiffness, K_1.

3 A second mass-isolator-mass test rig is constructed, with a source mass of M_2.

4 A single force is applied above the mount, and the resulting point and transfer mobilities are used to calculate the system's transmissibility via equation 4.

5 A transmissibility prediction is made for the second test rig using the stiffness obtained from the first test rig. The terms in equation 5 thus become, $Z_s = K_1/j\omega$ and $Z_m = j\omega M_2$.

* Both masses were chosen such that they were sufficiently different without having to worry about the introduction of preload effects on the isolator.

The process was repeated with the roles of M_1 and M_2 swapped. The results of this validation are shown in figure 4.
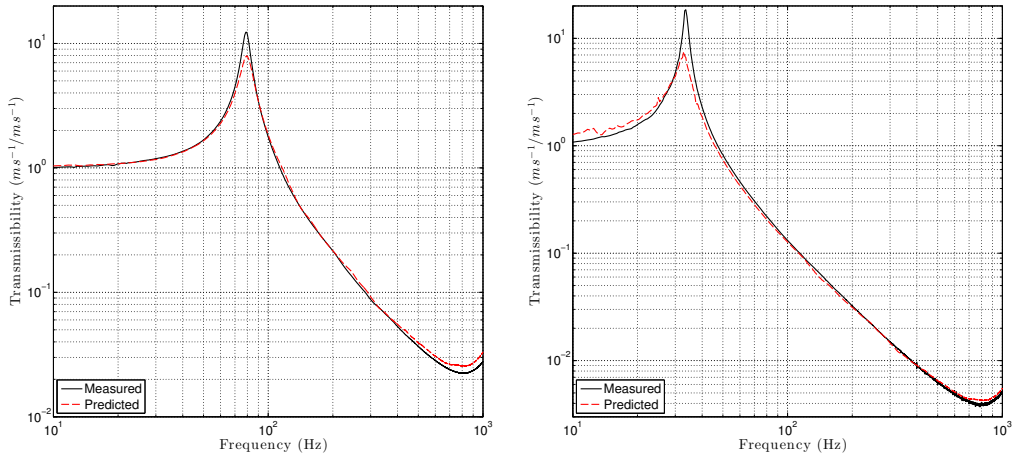
(a) Transmissibility of M_1 assembly, stiffness from M_2.

(b) Transmissibility of M_2 assembly, stiffness from M_1.

Figure 4: Measured and predicted transmissibility for two M-I-M assemblies.

It can be seen that in both cases the frequency at which the transmissibility peaks is predicted with considerable accuracy. The variation in amplitude between the measured

7

and predicted results may most likely be put down to the simplified nature of the mass on a spring model. Regardless of this difference in amplitude it has been shown that the stiffness obtained from one assembly may be used to predict the response of another. This not only confirms the transferability of the data, but also that it is in fact the true stiffness of the mount.

2.2 Rotational Components

Although not always necessary, the inclusion of rotational DOF in a structure borne vibration prediction has at times shown to be an essential requirement [17]. It would therefore prove advantageous if some form of extension could be provided allowing the simultaneous measurement of both the translational and rotational components of the dynamic transfer stiffness. Such an extension is provided through the application of a finite difference approximation [18]. Employing such a method requires minimal additional measurement equipment, no cumbersome test apparatus and may be conducted in-situ with relative ease. For a single arbitrary point the finite difference method allows the translational, rotational and cross mobility terms to be approximated using the following set of equations:

$$Y_{vf} \approx \frac{Y_{v_1 f_1} + Y_{v_1 f_2} + Y_{v_2 f_1} + Y_{v_2 f_2}}{4} \tag{6}$$

$$Y_{\alpha f} \approx \frac{-Y_{v_1 f_1} + Y_{v_2 f_2}}{4\Delta} \tag{7}$$

$$Y_{v\Gamma} \approx \frac{-Y_{v_1 f_1} + Y_{v_2 f_2}}{4\Delta} \tag{8}$$

$$Y_{\alpha\Gamma} \approx \frac{Y_{v_1 f_1} - Y_{v_1 f_2} - Y_{v_2 f_1} + Y_{v_2 f_2}}{4\Delta^2} \tag{9}$$

where Δ represents the spacing between accelerometers and the central point. If we consider the contact interface mobility matrix measured on the test rig shown in figure 2, the finite difference method may be applied in a convenient manner by simply pre and post multiplying the interface mobility matrix by a transformation matrix, as show in equation 10,

$$
\begin{bmatrix}
Y_{v_1 f_1} & Y_{v_1 \Gamma_1} & Y_{v_1 f_2} & Y_{v_1 \Gamma_2} \\
Y_{\alpha_1 f_1} & Y_{\alpha_1 \Gamma_1} & Y_{\alpha_1 f_2} & Y_{\alpha_1 \Gamma_2} \\
Y_{v_2 f_1} & Y_{v_2 \Gamma_1} & Y_{v_2 f_2} & Y_{v_2 \Gamma_2} \\
Y_{\alpha_2 f_1} & Y_{\alpha_2 \Gamma_1} & Y_{\alpha_2 f_2} & Y_{\alpha_2 \Gamma_2}
\end{bmatrix}
= \mathbf{B}
\begin{bmatrix}
Y_{c_{11} c_{11}} & Y_{c_{11} c_{12}} & Y_{c_{11} c_{21}} & Y_{c_{11} c_{22}} \\
Y_{c_{12} c_{11}} & Y_{c_{12} c_{12}} & Y_{c_{12} c_{21}} & Y_{c_{12} c_{22}} \\
Y_{c_{21} c_{11}} & Y_{c_{21} c_{12}} & Y_{c_{21} c_{21}} & Y_{c_{21} c_{22}} \\
Y_{c_{22} c_{11}} & Y_{c_{22} c_{12}} & Y_{c_{22} c_{21}} & Y_{c_{22} c_{22}}
\end{bmatrix}
\mathbf{B}^T \tag{10}
$$

where,

$$\mathbf{B} = \begin{bmatrix} \frac{1}{2} & \frac{1}{2} & 0 & 0 \\ \frac{-1}{2\Delta} & \frac{1}{2\Delta} & 0 & 0 \\ 0 & 0 & \frac{1}{2} & \frac{1}{2} \\ 0 & 0 & \frac{-1}{2\Delta} & \frac{1}{2\Delta} \end{bmatrix}. \tag{11}$$

The resulting mobility matrix may then be inverted and differentiated to obtain the translation, rotational and cross dynamic transfer stiffnesses.

Three more M-I-M test rigs were constructed (test rigs 3, 4 & 5), the details of which are given in table 1, and their contact interface mobilities measured. Using the finite difference method the transfer stiffness corresponding to an applied angular displacement at the top of the mount and a resultant torque at the bottom, $K_{\Gamma_2\alpha_1}$, was obtained. The results of which are shown in figure 5. It can be seen that as with the translational stiffness, the rotational stiffness remains relatively unchanged whilst the mobility can be seen to vary considerably, as expected. It is clear however, that at the lower frequencies the agreement between the results obtained for the rotational stiffness are less convincing than that of the translational stiffness. It is believed that this is partly due to the error introduced in the finite difference approximation, and that these results may be improved by optimising the accelerometer and force spacing used.
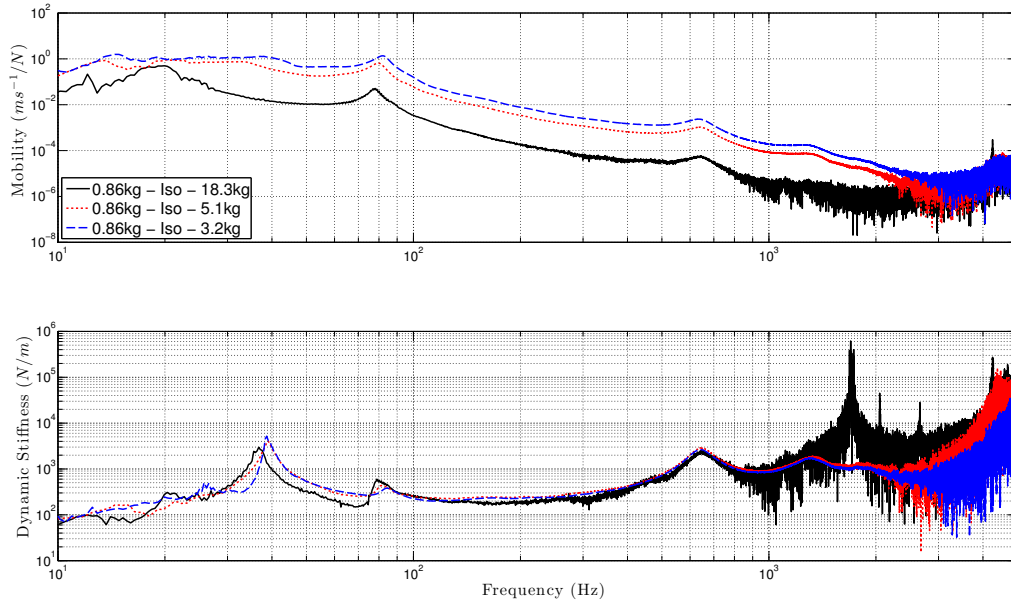
Figure 5: Results obtained from test rigs 3, 4 & 5. Upper - rotational transfer mobilities. Lower - rotational dynamic transfer stiffness's.

3   In-situ Dynamic Stiffness

It has so far been shown that the dynamic transfer stiffness of a resilient element may be obtained from a set of simple measurements on a M-I-M assembly with promising results. However, such systems are rarely found in practise, and it is therefore of interest to see how well the proposed method fares under a more realistic scenario. Let us now consider the beam-isolator-plate (B-I-P) assembly shown in figure 6. Details of this test rig may be found in table 1. The highly resonant nature of this assembly provides a challenging case, similar to something that may be encountered in practise.
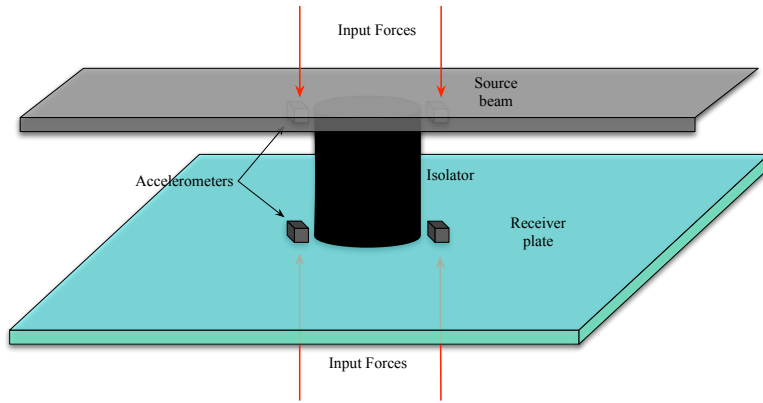
Figure 6: Beam-Isolator-Plate test rig.

The dynamic stiffness obtained from the measured B-I-P interface mobility matrix is shown in figure 7. It can be seen to agree well with the stiffness obtained from the mass-isolator-mass assembly over the majority of its frequency range. Although it is clear that the resonant nature of the assembly introduces a degree of error most notably around 600Hz, where the antiresonance of the system's mobility occurs. This error is thought to be a result of the measurement method used. Since we are unable to measure both the acceleration and applied force at the same position simultaneously we have had to adopt a spaced pair measurement configuration. The interface mobility matrix is then approximated by averaging these spaced pair mobilities above and below the mount. It is believed that this approximation introduces an error, most notable about the antiresonances of the system due to their dependance on excitation position, although it is believed that this error may be reduced by using a smaller separation distance. Regardless of this error the result does confirm the method's applicability to more 'realistic' assemblies.
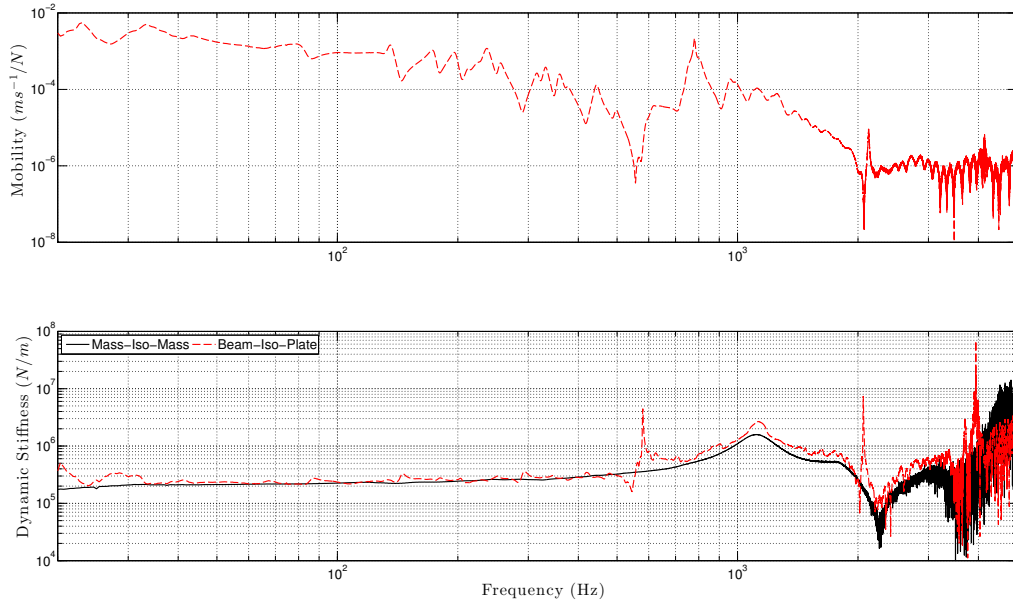
11

Figure 7: Results obtained from test rig 6. Upper - transfer mobility. Lower - dynamic transfer stiffness's (including stiffness obtained from test rig 1).

3.1 Remote Extension

One of the primary advantages of the method presented here is its ability to be applied in-situ on an assembly, without having to remove the resilient elements thus maintaining representative mounting conditions. However, with the advantage of in-situ application comes the disadvantage of restricted access. Often when conducting in-situ measurements, access is limited and the practitioner may be unable to excite the structure at the required interface contact points. In such cases it would be useful to allow the use of remote measurement positions. Such an extension is achieved via the application of the 'round trip' method. It has been shown by Moorhouse et al. [19,20] that the point and transfer mobilities across a single interface may be obtained without the need for excitation at the points of interest. Instead excitations are provided across two sets of remote measurement positions. The relationship of interest is given by,

$$\mathbf{Y_{cc}} = \mathbf{Y_{ca}} \mathbf{Y_{ab}^{-1}} \mathbf{Y_{cb}^{T}}. \tag{12}$$

Following a similar derivation to that of [20], whilst accounting for a second interface provides a means of obtaining the transfer mobility between two interfaces. The resulting relationship is given by,

$$\mathbf{Y}_{\mathbf{c_1 c_2}} = \mathbf{Y}_{\mathbf{c_1 a}} \mathbf{Y}_{\mathbf{ab}}^{-1} \mathbf{Y}_{\mathbf{c_2 b}}^{\mathbf{T}}. \tag{13}$$

Together equation 12 and 13 may be used to calculate each component of the interface mobility matrix,

$$\mathbf{Y}_{\mathbf{c_1 c_1}} = \mathbf{Y}_{\mathbf{c_1 a}} \mathbf{Y}_{\mathbf{ba}}^{-1} \mathbf{Y}_{\mathbf{c_1 b}}^{\mathbf{T}} \tag{14}$$

$$\mathbf{Y}_{\mathbf{c_1 c_2}} = \mathbf{Y}_{\mathbf{c_1 b}} \mathbf{Y}_{\mathbf{ab}}^{-1} \mathbf{Y}_{\mathbf{c_2 a}}^{\mathbf{T}} \tag{15}$$

$$\mathbf{Y}_{\mathbf{c_2 c_1}} = \mathbf{Y}_{\mathbf{c_2 a}} \mathbf{Y}_{\mathbf{ba}}^{-1} \mathbf{Y}_{\mathbf{c_1 b}}^{\mathbf{T}} \tag{16}$$

$$\mathbf{Y}_{\mathbf{c_2 c_2}} = \mathbf{Y}_{\mathbf{c_2 a}} \mathbf{Y}_{\mathbf{ba}}^{-1} \mathbf{Y}_{\mathbf{c_2 b}}^{\mathbf{T}}. \tag{17}$$

The above set of equations may be factorised into a single matrix equation and written in the more convenient form:

$$\begin{bmatrix} \mathbf{Y}_{\mathbf{c_1 c_1}} & \mathbf{Y}_{\mathbf{c_1 c_2}} \\ \mathbf{Y}_{\mathbf{c_2 c_1}} & \mathbf{Y}_{\mathbf{c_2 c_2}} \end{bmatrix} = \begin{bmatrix} \mathbf{Y}_{\mathbf{c_1 b}} & 0 \\ 0 & \mathbf{Y}_{\mathbf{c_2 a}} \end{bmatrix} \begin{bmatrix} \mathbf{Y}_{\mathbf{ab}} & 0 \\ 0 & \mathbf{Y}_{\mathbf{ba}} \end{bmatrix}^{-1} \begin{bmatrix} \mathbf{Y}_{\mathbf{c_1 a}}^{\mathbf{T}} & \mathbf{Y}_{\mathbf{c_2 a}}^{\mathbf{T}} \\ \mathbf{Y}_{\mathbf{c_1 b}}^{\mathbf{T}} & \mathbf{Y}_{\mathbf{c_2 b}}^{\mathbf{T}} \end{bmatrix} \tag{18}$$

The remote extension presented above has been applied to the same B-I-P assembly as shown in figures 6 and 7. An illustration of the remote measurement setup is shown in figure 8. The measurement positions on the source beam represent the remote points a and those on the receiver plate the remote points b. The measurement of the applied forces at these remote positions along with the resultant accelerations, including those at the interface contact points allow us to obtain all of the mobilities required by equation 18. It should be noted that three measurement positions were included in a to allow for the over-determination of the problem and that a determined solution only requires one remote measurement above and below the mount.
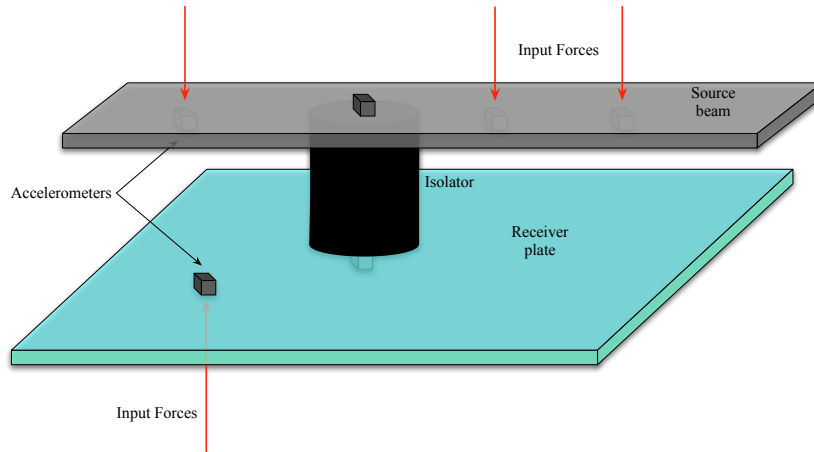
Figure 8: Beam-Isolator-Plate test rig showing remote measurement positions.

The inversion and differentiation of the resulting mobility matrix provides the dynamic transfer stiffness without ever having to excite at the contact interfaces. Results for both the determined and over-determined system are presented in figure 9 along side the results obtained from the direct (non-remote) M-I-M and B-I-P assemblies.

First considering the determined result, it can be seen that the resultant stiffness agrees well with that obtained from the M-I-M assembly across the majority of the frequency range. Similarly to the non-remote B-I-P stiffness there is a considerable amount of error at around 600Hz. Unlike the two non-remote results the bandwidth of the remote method is limited by the introduction of noise above 2kHz.
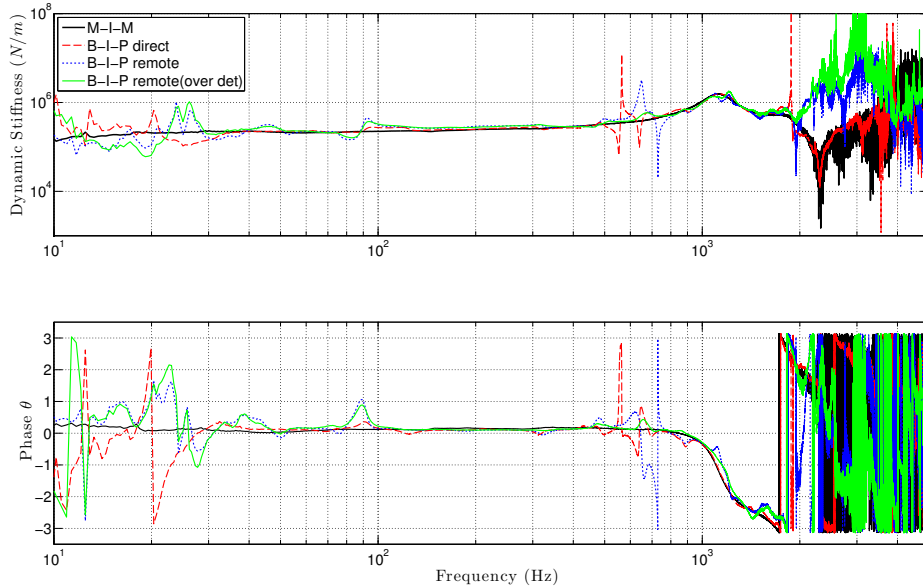
Figure 9: Remote results obtained from test rig 6. Upper - dynamic transfer stiffness's. Lower - corresponding phase responses.

Turning our attention to the over-determined result, it can be seen that the error introduced due to the system antiresonance is no longer visible. It is believed that the use of an over-determined remote mobility measurement returns a interface mobility with minimal error since no spatial averages are required and that this consequently reduced the error in the inversion.

4 Conclusion

An in-situ measurement method has been presented for the attainment of the dynamic transfer stiffness of resilient elements. Validation was provided through two simplified transmissibility predictions. It has been shown that the method provides good results over a considerable frequency range for simplistic non-resonant structures and may easily be extended to cater for rotational stiffness components via a finite difference approximation. The application of the method to more realistic resonant structures is slightly hampered by the introduction of measurement error about the system's anti-resonances. However, it is shown that this error may be remedied by using an extension to cater for remote measurement positions, thus providing the user with the opportunity to over-

15

determine the problem.

5 Acknowledgments

References

[1] Andy Moorhouse, Andrew S. Elliot, and YongHwa Heo. Intrinsic characterisation of structure-borne sound sources and isolators from in-situ measurements. In *Proceedings of Meetings on Acoustics*, volume 19, 2013.

[2] W.C Hurty. Dynamic analysis of structural systems using component modes. *AIAA Journal*, 3(4):678–685, 1965.

[3] M.C.C Bampton and R.R Craig. Coupling of substructures for dynamic analyses. *AIAA Journal*, 6(7):1313–1319, 1968.

[4] SN Voormeeren. *Dynamic substructuring methodologies for integrated dynamic analysis of wind turbines*. PhD thesis, TU Delft, 2012.

[5] D. De Klerk, D. J. Rixen, and S. N. Voormeeren. General Framework for Dynamic Substructuring: History, Review and Classification of Techniques. *AIAA Journal*, 46(5):1169–1181, May 2008.

[6] Matthew S. Allen, Randall L. Mayes, and Elizabeth J. Bergman. Experimental modal substructuring to couple and uncouple substructures with flexible fixtures and multi-point connections. *Journal of Sound and Vibration*, 329(23):4891–4906, November 2010.

[7] International Organization for Standardization. BS EN ISO 10846-1:2008 Acoustics and vibration - Laboratory measurement of vibroacoustic transfer properties of resilient elements, Part 1: Principles and guidelines, 2008.

[8] Leif Kari. Dynamic transfer stiffness measurements of vibration isolators in the audible frequency range. *Noise Control Engineering Journal*, 49(2):88–102, 2001.

[9] Lu Ean Ooi and Zaidi Mohd Ripin. Dynamic stiffness and loss factor measurement of engine rubber mount by impact test. *Materials & Design*, 32(4):1880–1887, April 2011.

[10] DJ Thompson, WJ Van Vliet, and JW Verheij. Developments of the indirect method for measuring the high frequency dynamic stiffness of resilient elements. *Journal of Sound and Vibration*, 213(1):169–188, 1998.

[11] Tian Ran Lin, Nabil H. Farag, and Jie Pan. Evaluation of frequency dependent rubber mount stiffness and damping by impact test. *Applied Acoustics*, 66(7):829–844, July 2005.

[12] International Organization for Standardization. BS EN ISO 10846-2:2008 Acoustics and vibration - Laboratory measurement of vibro-acoustic transfer properties of resilient elements, Part 2: Direct method for determination of the dynamic stiffness of resilient supports for translatory motion, 2008.

[13] International Organization for Standardization. BS EN ISO 10846-3:2002 Acoustics and vibration - Laboratory measurement of vibro-acoustic transfer properties of resilient elements, Part 3: Indirect method for determination of the dynamic stiffness of resilient supports for translatory motion, 2002.

[14] International Organization for Standardization. BS EN ISO 10846-4:2003 Acoustics and vibration - Laboratory measurement of vibro-acoustic transfer properties of resilient elements, Part 4: Dynamic stiffness of elements other than resilient supports for translatory motion, 2003.

[15] International Organization for Standardization. BS EN ISO 10846-5:2009 Acoustics and vibration - Laboratory measurement of vibro-acoustic transfer properties of resilient elements, Part 5: Driving point method for determination of the low-frequency transfer stiffness of resilient supports for translat, 2009.

[16] GJ O'Hara. Mechanical impedance and mobility concepts. *The journal of the Acoustical Society of America*, 41(5):1180–1184, 1967.

[17] Andrew. S Elliott. *Characterisation of structure borne sound sources in-situ.* PhD thesis, University of Salford, 2009.

[18] A.S Elliott, A.T Moorhouse, and G Pavić. Moment excitation and the measurement of moment mobilities. *Journal of sound and vibration*, 331(1):2499–2519, 2012.

[19] A.T. Moorhouse, T.A. Evans, and A.S. Elliott. Some relationships for coupled structures and their application to measurement of structural dynamic properties in situ. *Mechanical Systems and Signal Processing*, 25(5):1574–1584, July 2011.

17

[20] Andy Moorhouse and Andy Elliott. The "round trip" theory for reconstruction of Green's functions at passive locations. *The Journal of the Acoustical Society of America*, 134(5):3605–3612, November 2013.